Progress In Electromagnetics Research Letters, Vol. 109, 23–30, 2023

Design of a Planar Compact Dual-Band Bandpass Filter with Multiple Transmission Zeros Using a Stub-Loaded Structure

Guang Yong Wei[1], Yun Xiu Wang[1, *], Jie Liu[1, 2], and Hai Ping Li[1]

Abstract—This paper presents a new compact dual-band bandpass filter (BPF) with a stub-loaded resonator structure that can independently change its operating band to support GSM and WiFi applications for modern wireless communications. A short-circuit stub with a metal through hole is placed into the symmetrical resonator together with a pair of step impedance stubs and a pair of uniform open-circuit stubs. Inside the resonator, the open stubs fold in on themselves, minimizing the circuit for integration with other parts and enhancing the selectivity of the filter. Even-odd mode theory can be employed to investigate the circuit because of the resonator geometric symmetry. The first and second operational frequency bands can then be built using the calculated odd and even mode frequencies to match our requirements. The manufactured experimental dual-band filter is compared to the simulation results, and the statistics revealed good agreement. The calculated structural measures $0.13\lambda_g \times 0.1\lambda_g$.

1. INTRODUCTION

With the vigorous development of modern wireless communication technology, the demand for multi-band bandpass filters in communication is increasing. As an essential component of the RF front end, filters provide high-quality filtered signals for the required equipment. In order to make it have excellent performance of small circuit size and high passband selectivity, researchers have developed a variety of bandpass filters [1–6]. As a result, numerous compact dual-band bandpass filters based on various technologies, including stub-loaded resonators (SLRs) [7], ring resonators [8], defected ground structures (DGSs) [9, 10], and stepped impedance resonators coupling techniques [11], have been developed in recent years. [12] describes the construction of a square ring resonator-based dual-band bandpass filter made of two opposing square rings connected by open-circuited stubs at their ends. Because it uses two resonators and is not precisely symmetrical, it has a greater circuit area. Similar dual-band bandpass filters are designed in [13] and [14] using the stepped impedance resonator coupling technique and the backside etched defect ground structure (DGS) of the dielectric substrate, but the presented filters also have a larger circuit size and an untunable passband.

The primary goal of this work is to propose an advanced dual-band bandpass microwave filter for GSM and WiFi applications, which has a simple structure, passbands that are easily adjusted, and enhanced filter selectivity with numerous transmission zeros (TZs) in the stopband. The proposed BPF configuration is based on the construction of the stub-loaded resonator. The even-odd mode approach is initially employed to investigate the resonator, after which the necessary even-odd mode frequencies are determined from the disassembled individual circuits. Secondly, the impacts of resonator symmetric opencircuited stubs and the middle shortcircuited stubs on the dual-band bandwidth and the stopband transmission zeros are described. The effect of the feed line on the in-band performance and other

Received 26 December 2022, Accepted 22 January 2023, Scheduled 1 February 2023
* Corresponding author: Yun Xiu Wang (627662147@qq.com).
[1] School of Electronic and Information Engineering, China West Normal University, Nanchong 637009, China. [2] School of Physics and Astronomy, China West Normal University, Nanchong 637009, China.

relevant parameters was then investigated. Finally, a prototype dual-band BPF is manufactured and measured to confirm the performance of the proposed filter.

2. STUB-LOADED STRUCTURAL ANALYSIS

In Fig. 1, a simple stub-loaded resonator with two pairs of open-circuited stubs, one pair of stepped impedance open-circuited stubs (SIOSs), and one short-circuited stub in the middle is shown. This structure is symmetrical; therefore, the odd-even mode analysis technique can decompose the stub-loaded resonator in Fig. 1(a) into Fig. 1(b) even mode circuit and (c) odd mode circuit. The six resonant circuits for this even-odd mode are shown in Figs. 1(d) through 1(i), respectively.

Now, using the fundamental microwave circuit theory [15] to get the total input admittance:

$$Y_{in} = Y_o \frac{Y_L + jY_o \tan\theta}{Y_o + jY_L \tan\theta} \tag{1}$$

where $\theta = \beta L$ is the electrical length of the stubs; $\beta = 2\pi/\lambda_g$ is the propagation constant; λ_g is the guided wavelength. We determine the input admittance $Y_{in,even1}$ and the resonant frequency f_{even1} from Fig. 1(d). First, take into account the short-circuited stub "L_s" so $Y_L = \infty$. The following Equation (2) can be obtained by inserting Y_L and $Y = Y_s/2$ into previously mentioned Equation (1):

$$Y_{ins} = -j\left(\frac{Y_s}{2}\right)\cot\theta_s \tag{2}$$

where Y_{ins} is the short-circuited stub's input admittance, and L_s is its length. Equation (1) can be used to determine the value of Y_{ins} and $Y = Y_1$, giving us $Y_{in,even1}$ as:

$$Y_{in,even1} = -jY_1 \frac{Y_s - 2Y_1 \tan(\theta_1+\theta_2+\theta_3)\tan(\theta_s)}{2Y_1 \tan(\theta_s) + Y_s \tan(\theta_1+\theta_2+\theta_3)} \tag{3}$$

where $\theta_1 = \beta L_1$, $\theta_2 = \beta L_2$, $\theta_3 = \beta L_3$, $\theta_s = \beta L_s$, and assume $Y_s/2 = Y_1$. According to resonance conditions $Y_{in,even1} = 0$, the following even mode resonance frequency f_{even1} can be obtained:

$$f_{even1} = \frac{(2n-1)c}{4(L_1+L_2+L_3+L_s)\sqrt{\varepsilon_{eff}}} \tag{4}$$

where $n = 1, 2, 3, \ldots$, c represents the light speed in vacuum, and ε_{eff} shows the effective permittivity of the substrate which is given by:

$$\varepsilon_{eff} = \frac{1+\varepsilon_r}{2} + \frac{\varepsilon_r - 1}{2} \times \frac{1}{\sqrt{1+12\dfrac{h}{w}}} \tag{5}$$

where w and h are the dimensions of the dielectric substrate, and ε_r is the relative permittivity. The resonator symmetry plane is also shorted for the odd-mode, with $Y_L = \infty$, $Y_1 = Y_0$. Using Fig. 1(e), we can also obtain the odd-mode admittance $Y_{in,odd1}$:

$$Y_{in,odd1} = \frac{Y_1}{j\tan(\theta_1+\theta_2+\theta_3)} \tag{6}$$

Because the resonance condition is $Y_{in,odd1} = 0$, the corresponding oddmode expression can be obtained from Equation (6):

$$f_{odd1} = \frac{(2n-1)c}{4(L_1+L_2+L_3)\sqrt{\varepsilon_{eff}}} \tag{7}$$

The remaining even-odd mode frequencies can be derived using the same procedure as above using Figs. 1((f)–(i)):

$$Y_{in,even2} = -jY_4 \frac{Y_1 - Y_4 \tan\theta_4 \tan(\theta_2+\theta_3+\theta_s)}{Y_4 \tan(\theta_2+\theta_3+\theta_s) + Y_1 \tan(\theta_4)} \tag{8}$$

$$f_{even2} = \frac{(2n-1)c}{4(L_2+L_3+L_4+L_s)\sqrt{\varepsilon_{eff}}} \tag{9}$$

$$f_{odd2} = \frac{(2n-1)c}{4(L_2+L_3+L_4)\sqrt{\varepsilon_{eff}}} \tag{10}$$

$$f_{even3} = \frac{(2n-1)c}{4(L_3+L_5+L_6+L_s)\sqrt{\varepsilon_{eff}}} \tag{11}$$

$$f_{odd3} = \frac{(2n-1)c}{4(L_3+L_5+L_6)\sqrt{\varepsilon_{eff}}} \tag{12}$$

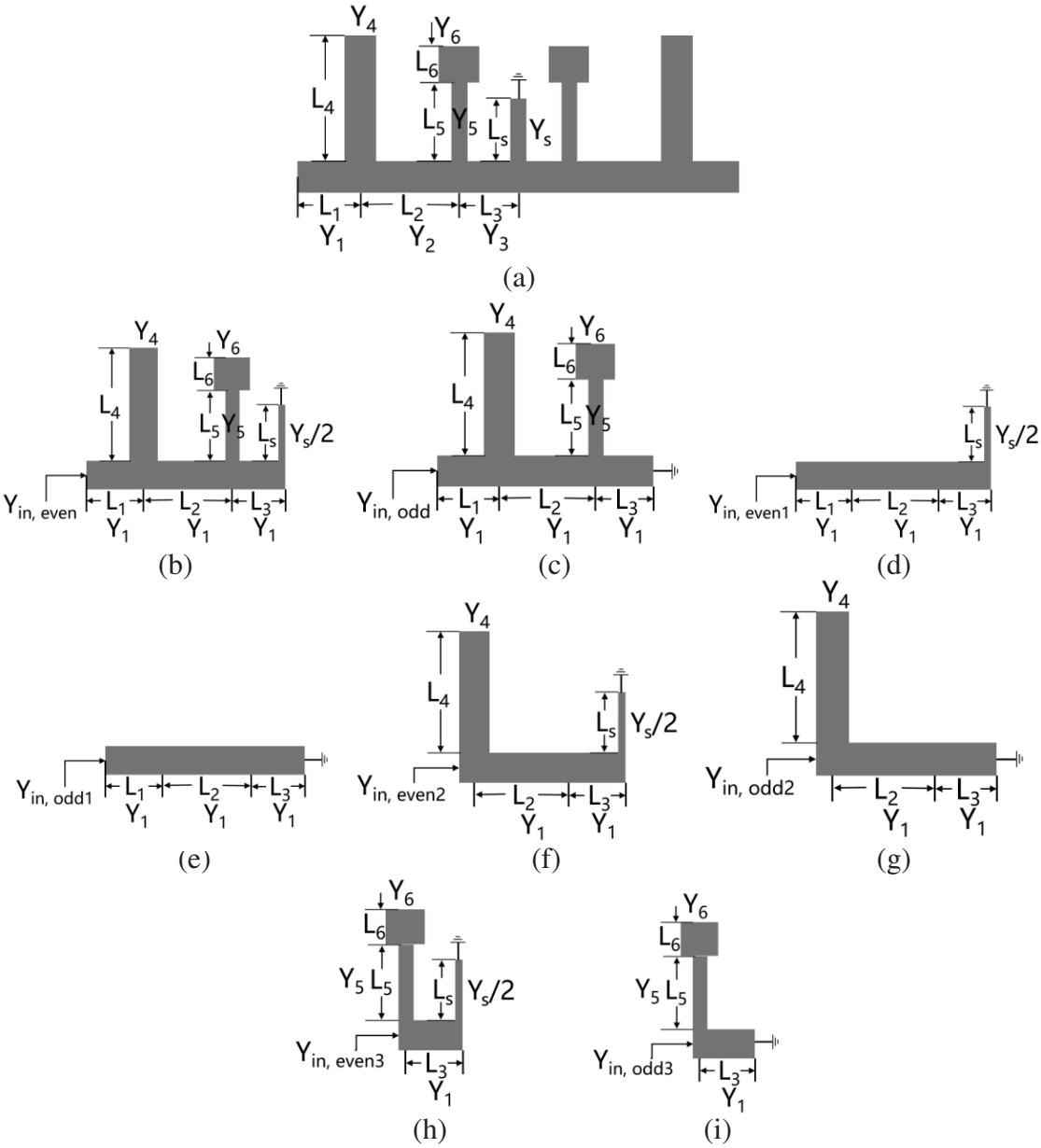

Figure 1. (a) Stub-loaded resonator. (b) and (c) Even and odd mode circuits. (d)–(i) Decomposition of (b) and (c).

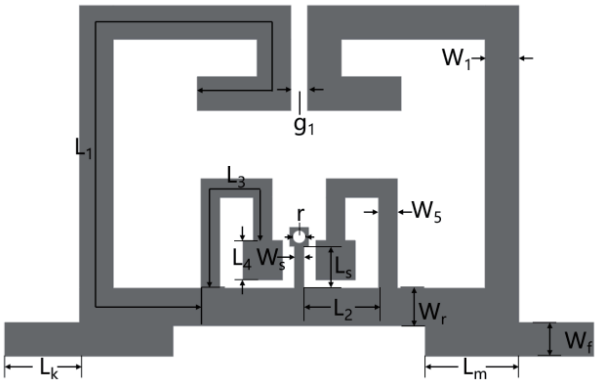

Figure 2. The proposed topology of dual-band BPF.

3. CALCULATING RESONANT FREQUENCIES

The aforementioned mathematical process is used to determine each resonator's physical size. In Fig. 2, a compact dual-band BPF is developed. Fig. 2 shows that the physical length of the parameter in the denominator of Equation (13) determines the even-mode frequency of the first passband that we calculate as follows:

$$f_{even,1} = \frac{(2n-1)c}{4(L_s + L_1 + L_2)\sqrt{\varepsilon_{eff}}} \tag{13}$$

Equation (13) asks for the corresponding length values and yields the frequency of the first even mode, which is $f_{even,1} = 0.79\,\text{GHz}$. The first passband consists of one even and one odd modes. The equation for $f_{odd,1}$ based on Fig. 2 is given below:

$$f_{odd,1} = \frac{(2n-1)c}{4\,(L_1 + L_2)\,\sqrt{\varepsilon_{eff}}} \tag{14}$$

by the same token, placing L_1 and L_2 into Equation (14) and get $f_{odd,1} = 1.17\,\text{GHz}$. Similarly, the even mode $f_{even,2}$ and odd mode $f_{odd,2}$ can be calculated by Equations (15) and (16), respectively.

$$f_{even,2} = \frac{(2n-1)c}{4\,(L_s + L_2 + L_3 + L_4)\,\sqrt{\varepsilon_{eff}}} \tag{15}$$

$$f_{odd,2} = \frac{(2n-1)c}{4\,(L_2 + L_3 + L_4)\,\sqrt{\varepsilon_{eff}}} \tag{16}$$

Equations (15) and (16) are used to estimate the even and odd resonator frequencies for the second passband, which are $f_{even,2} = 2.15\,\text{GHz}$ and $f_{odd,2} = 2.83\,\text{GHz}$, respectively. It is significant that the nearby resonators' magnetic coupling is what causes the minor shift in frequencies, and by using parametric analysis in electromagnetic simulation software, we may change them to fall within our target range.

4. PARAMETRIC STUDY

To verify the conclusion of the above analysis, the resonator parameters of interest were selected for the study. The first and second passbands are controlled by the length L_1, as illustrated in Fig. 3(a), and shifting the length from 37.1 mm to 39.1 mm will change the widths of the two frequency bands. The center frequency and position of transmission zeros T_{Z1} and T_{Z2} move to a lower frequency. Adjusting the parameter can adjust the first passband to the desired location. Additionally, the lower frequency of the second passband will be impacted by the movement of the two transmission zeros. As a result, while the first passband is altered, the transmission zeros T_{Z1} and T_{Z2} can be moved to alter the low frequency of the second passband.

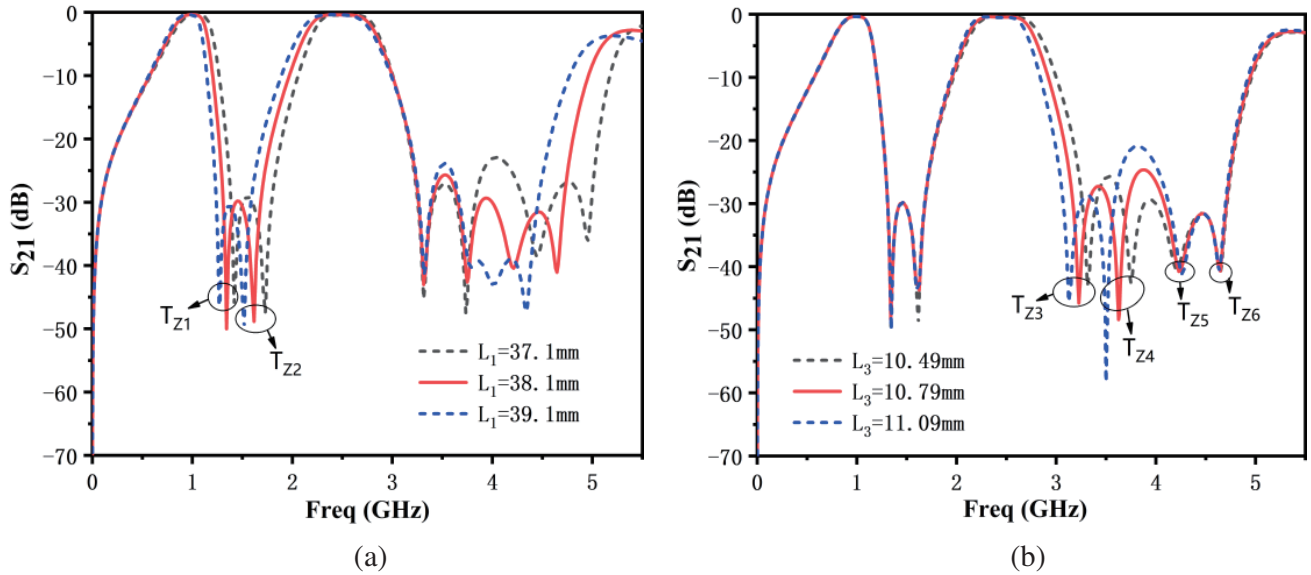

Figure 3. S_{21} frequency response of the dual-band BPF in case of varying (a) L_1 (b) L_3.

When the step impedance open-circuited stub length L_3 is raised from 10.49 mm to 11.09 mm, the frequency responses are shown in Fig. 3(b). The transmission zeros T_{Z3} and T_{Z4} change from a higher frequency to a lower frequency as the length of L_3 rises, while the transmission zeros T_{Z1}, T_{Z2}, T_{Z5}, and T_{Z6} almost remain fixed. This results in the center frequency of the second passband moving to a lower frequency. Therefore, by altering the length of L_3, the bandwidth of the second passband can be obtained. As a result, it is clear from the simulation results that the length of the resonator open-shorted stubs can be changed to alter both passbands of the proposed filter.

The second benefit is that by adjusting the parameter t (height of feeder to bottom of the resonator), the return loss in the passband may be controlled. As shown in Fig. 4(a), altering the parameter t will

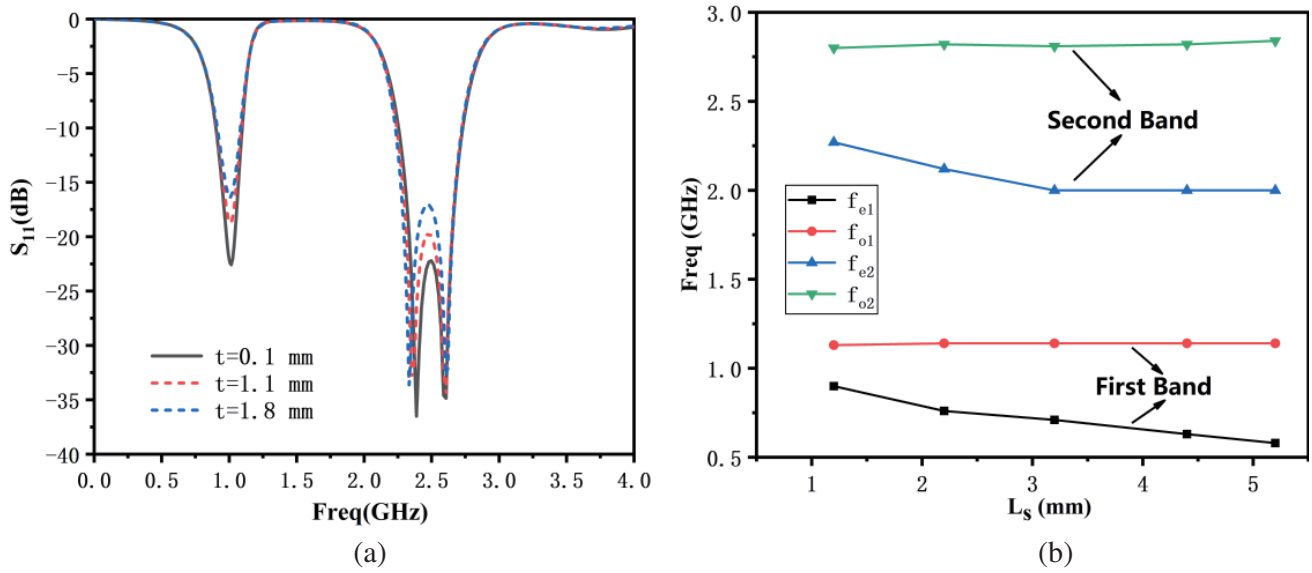

Figure 4. (a) The return loss of the filter for various values of t. (b) Simulated resonant modes for various values of L_s.

only have an impact on the return loss of the dual passbands; the bandwidth is unaffected. Fig. 4(b) depicts the resonant frequency distribution of various L_s lengths to investigate the impact of the short-circuited stub in the middle of the resonator on the filter. The two even-mode frequencies f_{e1} and f_{e2} migrate to a lower frequency as the stub length L_s is increased, but the two odd-mode frequencies f_{o1} and f_{o2} remain unchanged.

Determine the coupling coefficient "K_e" and external quality factor "Q_e" using the following equations [16]:

$$K_e = \frac{f_h^2 - f_l^2}{f_h^2 + f_l^2} \tag{17}$$

$$Q_e = \frac{\omega_0}{\Delta\omega_{(3\,\mathrm{dB})}} \tag{18}$$

where f_l and f_h show the lower and upper cutoff frequencies of the two passbands; ω_0 represents the central frequency; and $\omega_{(3\,\mathrm{dB})}$ represents the 3 dB absolute bandwidth centered at ω_0.

The suggested dual-band filter's electric coupling coefficient, which is plotted in Fig. 5(a), depends on the parameter "g_1". It is seen that the corresponding electric coupling decreases as the distance "g_1" grows. Equation (18), which is illustrated in Fig. 5(b) with the parameter "W_f" given from Fig. 2, also calculates the external quality factor of the filter.

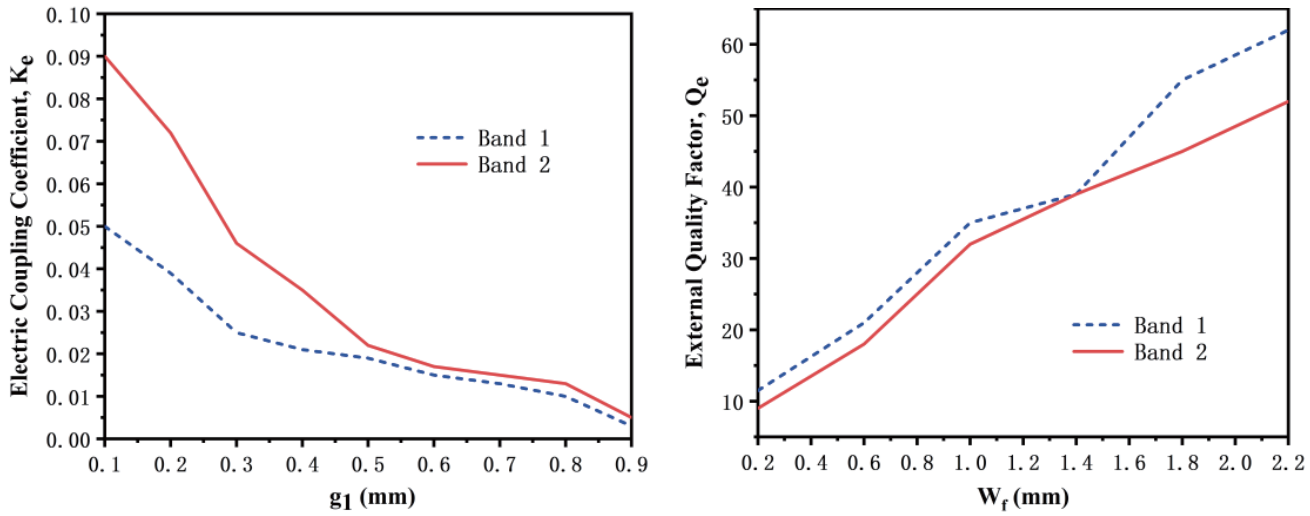

Figure 5. (a) Electric coupling coefficient "K_e" against g_1. (b) External quality factor "Q_e" against "W_f".

5. OPTIMIZED DESIGN AND FABRICATION OF THE BPF

The filter is simulated and optimized using electromagnetic simulation software ADS and adopting Agilent N5244A vector network analyzer to measure its parameter performance. The input and output ports must be 1.8 mm wide since we utilize an FR4 substrate with a 0.8 mm thickness. The optimized design parameters of the proposed filter are as follows: $L_1 = 38.17$, $L_2 = 4.1$, $L_3 = 10.79$, $L_4 = 2.1$, $L_m = 5.1$, $W_f = 1.8$, $W_1 = 1.81$, $W_r = 1.81$, $L_s = 2.25$, $W_5 = 1.02$, $r = 0.35$, $g_1 = 0.9$, $W_s = 0.5$, $t = 0.1$ (all dimensions are in mm). The image of the manufactured dual-band filter prototype is shown in Fig. 6. The size is only about 23.5 mm $\times$ 16.9 mm ($0.13\lambda_g \times 0.1\lambda_g$), where λ_g represents the guided wavelength. The simulated and measured transmission and reflection characteristics of the developed dual-band filter are shown in Fig. 7. The obvious reduction of in-band reflection in the second frequency band may be due to the influence of manufacturing error. The dual-band BPF operates at

0.94 GHz and 2.48 GHz, with corresponding 3 dB FBW values of 39% and 27%, respectively. All two passbands' insertion losses were measured at 0.28 dB and 0.92 dB at their respective center frequencies. To provide a high selectivity passband filter response, six transmission zeros are produced with more than 24 dB attenuation at the following frequencies: 1.32 GHz, 1.62 GHz, 3.3 GHz, 3.78 GHz, 4.08 GHz, and 4.68 GHz. In Table 1, dual-band BPF is compared to previous publications that have been published in the literature, and it is shown that the newly proposed filter has good qualities.

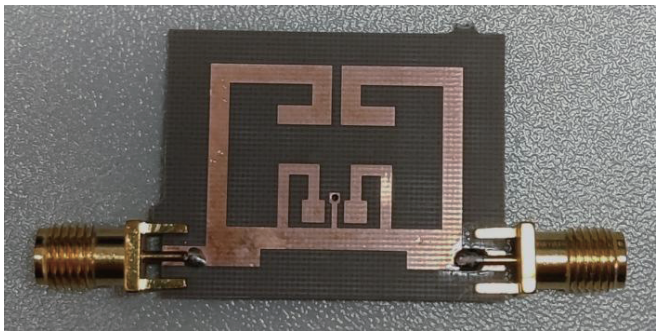

Figure 6. Photograph of fabricated filter prototype.

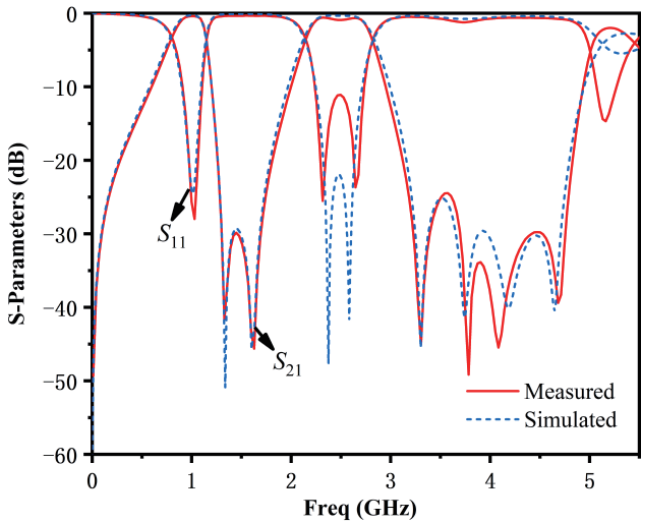

Figure 7. Simulated and measured responses of the filter.

Table 1. Comparisons with other proposed filters.

Ref.	Center freq. (GHz)	IL (dB)	3-dB FBW (%)	TZs	Circuit size ($\lambda_g \times \lambda_g$)
[9]	3.57/5.87	1.62/1.69	5.8/5.4	3	0.39×0.31
[11]	2.4/5.2	1.3/1.72	8/6	2	0.3×0.3
[12]	2.6/5.8	1.1/2.15	10.4/3.6	4	0.26×0.34
[13]	2.41/3.52	2/2.2	5.8/7.7	4	0.36×0.24
This work	0.94/2.48	0.28/0.92	39/27	6	0.13×0.1

6. CONCLUSION

A novel compact dualband BPF using multi-stubs is presented and measured. The even-odd mode approach is used to investigate the proposed BPF because of its symmetrical geometry. By controlling the physical parameters of the stub, it is easy to generate dual frequency bands and achieve multiple zeros in the stopband. The proposed BPF is tuned to operate at GSM-900, WiFi (2.4 GHz) bands. Both situations have excellent agreement between the measured and simulated results. This filter is a strong contender for wireless communication systems due to its affordable realization and adjustable transmission zeros.

REFERENCES

1. Karimzadeh-Jazi, R., M. A. Honarvar, and F. Khajeh-Khalili, "High Q-factor narrow-band bandpass filter using cylindrical dielectric resonators for X-band applications," *Progress In Electromagnetics Research Letters*, Vol. 77, 65–71, 2018.
2. Kumar, R. and S. N. Singh, "Design and analysis of ridge substrate integrated waveguide bandpass filter with octagonal complementary split ring resonator for suppression of higher order harmonics," *Progress In Electromagnetics Research C*, Vol. 89, 87–99, 2019.
3. Gorur, A. K., "A novel compact microstrip balun bandpass filter design using interdigital capacitor loaded open loop resonators," *Progress In Electromagnetics Research Letters*, Vol. 76, 47–53, 2018.
4. Wei, F., H. J. Yue, X. H. Zhang, and X.-W. Shi, "A balanced quad-band BPF with independently controllable frequencies and high selectivity," *IEEE Access*, Vol. 7, 110316–110322, 2019.
5. Yang, Q., Y.-C. Jiao, and Z. Zhang, "Compact multiband bandpass filter using low-pass filter combined with open stub-loaded shorted stub," *IEEE Transactions on Microwave Theory and Techniques*, Vol. 66, No. 4, 1926–1938, 2018.
6. Yin, B. and Z. Y. Lin, "A novel dual-band bandpass SIW filter loaded with modified dual-CSRRs and Z-shaped slot" *Int. J. of Electron. Commun.*, Vol. 121, 153–261, 2020.
7. Wang, Z. J., C. Wang, and N. Y. Kim, "Dual-/triple-wideband microstrip bandpass filter using independent triple-mode stub-loaded resonator" *Microwave and Optical Technology Letters*, Vol. 60, No. 1, 56–64, 2018.
8. Tang, M. C., T. Shi, S. Y. Chen, and H. L. Cao, "Dual-band bandpass filter based on a single triple-mode ring resonator," *Electron. Lett.*, Vol. 52, No. 9, 722–723, 2016.
9. Huang, W., L. Li, L. Li, Y. Ren, and Y. Ma, "A compact coplanar waveguide dual-band bandpass filters based on defected ground structures," *IEICE Electronics Express*, Vol. 18, No. 15, 16, 2021.
10. Lai, X., C. H. Liang, H. Di, and B. Wu, "Design of tri-band filter based on stub loaded resonator and DGS resonator," *IEEE Microwave and Wireless Components Letters*, Vol. 20, No. 5, 265–267, 2010.
11. Lu, H., Y. Yuan, J. Huang, X. Zhang, and N. Yuan, "Design of compact dual-mode dual-band microstrip bandpass filter using stepped-impedance resonator for wireless communication applications," *2018 International Conference on Microwave and Millimeter Wave Technology*, 1–3, 2018.
12. Ren, B., H. Liu, Z. Ma, M. Ohira, P. Wen, X. Wang, and X. Guan, "Compact dual-band differential bandpass filter using quadruple-mode stepped-impedance square ring loaded resonators," *IEEE Access*, Vol. 6, 21850–21858, 2018.
13. Song, K., F. Zhang, and Y. Fan, "Miniaturized dual-band bandpass filter with good frequency selectivity using SIR and DGS," *Int. J. of Electron. Commun.*, Vol. 68, No. 5, 384–387, 2014.
14. Zobeyri, M. R. and A. R. Eskandari, "Design of single- and dual-band BPFs using folded 0° feed structures and embedded resonators," *International Journal of Electronics and Communications*, Vol. 96, 18–29, 2018.
15. Pozar, D. M., *Microwave Engineering*, Wiley, Hoboken, NJ, USA, 2009.
16. Sami, A. and M. Rahman, "A very compact quintuple band bandpass filter using multimode stub loaded resonator," *Progress In Electromagnetics Research C*, Vol. 93, 211–222, 2019.